Epitaxial Growth of Full-Heusler Alloy Co_2MnSi Thin Films on MgO-Buffered MgO Substrates

H. Kijima, T. Ishikawa, T. Marukame, H. Koyama, K. Matsuda, T. Uemura, and M. Yamamoto

Division of Electronics for Informatics, Graduate School of Information Science and Technology, Hokkaido University, Sapporo 060–0814, Japan

Full-Heusler alloy Co_2MnSi (CMS) thin films were epitaxially grown on MgO-buffered MgO substrates through magnetron sputtering. The films were deposited at room temperature and subsequently annealed *in situ* at 600 °C. X-ray pole figure measurements of the annealed films showed 111 peaks with fourfold symmetry, providing direct evidence that these films were epitaxial and crystallized in the $L2_1$ structure. The annealed films had sufficiently flat surface morphologies with root-mean-square roughness of about 0.22 nm at a film thickness of 50 nm. The saturation magnetization of the annealed films was 4.5 μ_B/f.u. at 10 K, corresponding to about 90% of the Slater–Pauling value for CMS.

***Index Terms*—Co-based full-Heusler alloy, Co_2MnSi, epitaxial growth, half-metallic, MgO.**

I. Introduction

COBALT-BASED full-Heusler alloy thin films have recently attracted much interest as highly desirable ferromagnetic electrodes for spintronic devices [1]–[9]. This is because of the half-metallic ferromagnetic nature theoretically predicted for some of these alloys [10], [11] and because of their high Curie temperatures, which are well above room temperature (RT) [12]. We recently reported fully epitaxial magnetic tunnel junctions (MTJs) with a Co-based full-Heusler alloy thin film of either $Co_2Cr_{0.6}Fe_{0.4}Al$ (CCFA) or Co_2MnGe as a lower electrode and a MgO tunnel barrier and obtained relatively high tunnel magnetoresistance (TMR) ratios at RT for these epitaxial MTJs (e.g., 42% for CCFA-MTJs at RT) [3], [6], [8]. One Co-based full-Heusler alloy in particular, Co_2MnSi (CMS), has attracted interest because of the large energy gap of ~ 0.42 eV theoretically predicted for its minority spin band [10] and its high Curie temperature of 985 K [12]. Recently, epitaxial CMS thin films have been grown on GaAs (001) by pulsed laser deposition [4] and on Cr-buffered MgO substrates by magnetron sputtering [5]. TMR ratios of 70% at RT and 159% at 2 K have been reported for MTJs using an epitaxial CMS film grown on a Cr-buffered MgO substrate as a lower ferromagnetic electrode and having an amorphous AlO_x tunnel barrier [5]. The lattice mismatch between CMS and MgO for 45° in-plane rotation is -5.1%, which is larger than the mismatch of -2.0% between CMS and Cr. However, epitaxial growth of CMS films on a MgO buffer layer will lead to fully epitaxial MTJs consisting of CMS lower and upper electrodes and a MgO tunnel barrier. Our goal in this work has therefore been to fabricate epitaxial CMS films on MgO-buffered MgO substrates applicable for fully epitaxial magnetic tunnel junctions with a MgO tunnel barrier and then to clarify the structural and magnetic properties of the fabricated CMS films.

II. Experimental Methods

Each layer in the MgO/CMS bilayer structure (a CMS thin film on a MgO buffer layer) was successively deposited in an ultrahigh vacuum chamber (with a base pressure of around 8×10^{-8} Pa) through the combined use of magnetron sputtering and electron beam evaporation. A 10-nm-thick MgO buffer layer was first deposited on the MgO(001) single-crystal substrate at 400 °C by electron beam evaporation to reduce or eliminate surface defects and microscopic roughness. The CMS film was then deposited on the MgO buffer layer at RT by rf magnetron sputtering with Ar as a sputtering gas, and subsequently annealed *in situ* at 200 to 600 °C for 15 min. The CMS film composition was analyzed using inductively coupled plasma optical emission spectroscopy for a 100-nm-thick CMS film deposited at RT. It was found to be $Co_{2.00}Mn_{0.84}Si_{0.80}$ with an accuracy of 2%–3% for each element.

We investigated the structural properties of the fabricated CMS films through X-ray Bragg scans and X-ray pole figure measurements (Bruker AXS D8 DISCOVER Hybrid). Reflection high-energy electron diffraction (RHEED) patterns were observed *in situ* for each successive layer of the bilayer structure. The surface morphologies were observed using atomic force microscopy (Digital Instruments). The magnetic properties were measured using a superconducting quantum interference device magnetometer (Quantum Design MPMS) at temperatures from RT to 10 K. For the estimation of magnetization, the contribution from the MgO substrate was subtracted.

III. Experimental Results and Discussion

Fig. 1 shows RHEED patterns, along the azimuths of $[100]_{MgO}$ and $[110]_{MgO}$ (corresponding to $[110]_{CMS}$ and $[100]_{CMS}$, respectively), obtained *in situ* for each successive layer in the MgO/CMS bilayer structure. The streak patterns were dependent on the electron injection direction for an as-deposited CMS film [Fig. 1(b)], indicating that the film grew epitaxially. It was the same for the CMS film postdeposition annealed *in situ* at 600 °C. The streak patterns of the annealed CMS film [Fig. 1(c)] were sharper and more distinct than those

Digital Object Identifier 10.1109/TMAG.2006.878850

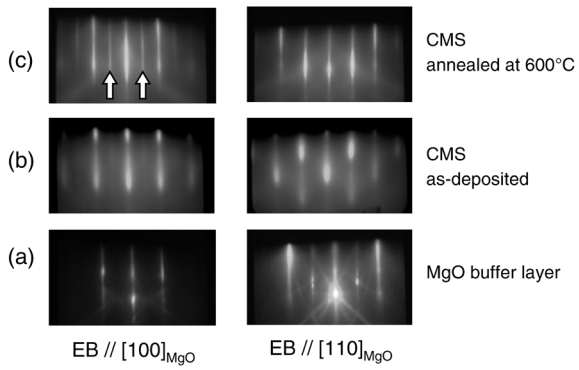

Fig. 1. RHEED patterns, along the azimuths of $[100]_{\mathrm{MgO}}$ and $[110]_{\mathrm{MgO}}$ (corresponding to $[110]_{\mathrm{CMS}}$ and $[100]_{\mathrm{CMS}}$, respectively), for each successive layer: (a) MgO buffer layer (10 nm); (b) a CMS film (50 nm) grown at RT; and (c) a CMS film annealed at 600 °C after deposition. In (c), the CMS film annealed at 600 °C shows additional streak patterns (indicated by arrows), showing that the 600 °C-annealed CMS film had the $\mathrm{L2_1}$ structure.

of the as-deposited film [Fig. 1(b)]. This indicates that the surface flatness of the CMS film deposited at RT was improved by the postdeposition annealing at 600 °C, which is consistent with the AFM observations of the surface morphologies described below. Furthermore, we observed $1/2$-order superlattice reflections along the $[110]_{\mathrm{CMS}}$ direction in the RHEED patterns for the CMS film annealed at 600 °C [indicated by the arrows in Fig. 1(c)], showing that this CMS film had the $\mathrm{L2_1}$ structure.

Fig. 2(a) shows X-ray θ-2θ diffraction patterns of 50-nm-thick CMS films as-deposited and postdeposition annealed at temperatures ranging from 200 to 600 °C. As Fig. 2(a) shows, 002 and 004 peaks were clearly observed even for the as-deposited CMS film. The intensities of the 002 and 004 peaks were increased by postdeposition annealing at 200 to 600 °C. In this sense, the crystal structure of the as-deposited CMS film was improved by the annealing.

An X-ray pole figure scan of a CMS film deposited at RT and subsequently annealed at 600 °C is shown in Fig. 2(c) along with that of a MgO substrate. In this figure, we set the MgO [100] direction as the origin of the sample rotation angle φ. As can be seen in Fig. 2(c), CMS 111 diffraction peaks with fourfold symmetry with respect to φ were clearly observed at a tilt angle χ of 54.7°. This provides direct evidence that the 600 °C-annealed film was epitaxial and crystallized in the $\mathrm{L2_1}$ structure. Because the φ values for the CMS 111 peaks were shifted by 45° with respect to those of the MgO 111 peaks, the crystallographic relationship was CMS (001)[100]||MgO (001)[110]. In contrast, in the X-ray pole figure scans for the as-deposited CMS thin films, 022 peaks were observed with fourfold symmetry with respect to φ, while 111 peaks were not observed. These results along with the observation of the 002 peak in the X-ray θ-2θ scan described above show that as-deposited CMS films also grew epitaxially, but with the B2 or a mixture of the B2 and A2 structures, where the B2 structure implies disorder in the atomic arrangement between Mn and Si, and the A2 structure implies disorder in all of the atomic arrangement. Annealing the as-deposited CMS film at temperatures ranging from 400 to 600 °C caused 111 peaks specific to the $\mathrm{L2_1}$ structure to appear and their intensity rose with increasing annealing temperature.

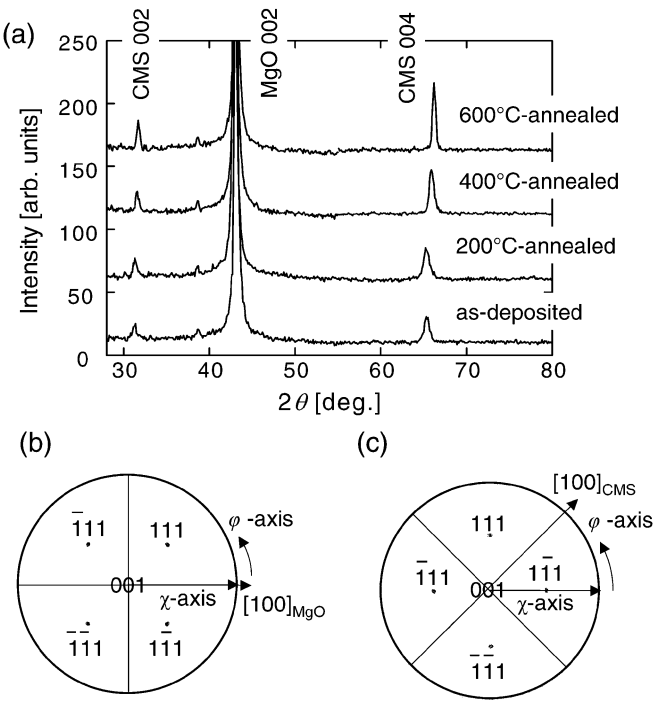

Fig. 2. (a) X-ray θ-2θ diffraction patterns of 50-nm-thick CMS films as-deposited and postdeposition annealed at 200–600 °C. (b) and (c) X-ray pole figures of (b) MgO 111 and (c) CMS 111 for a CMS film annealed at 600 °C.

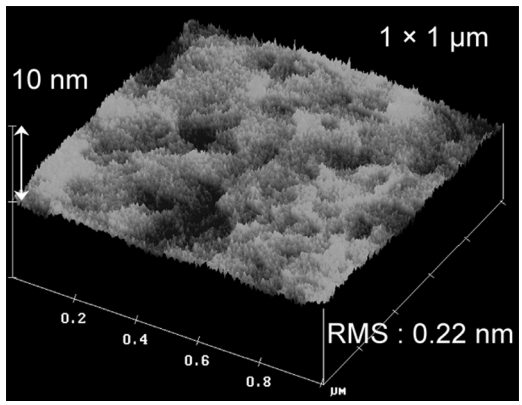

Fig. 3. Three-dimensional AFM image ($1 \times 1\,\mu\mathrm{m}$) of the surface topography of a 50-nm-thick CMS thin film annealed at 600 °C after deposition.

To fabricate high-quality MTJs, a lower ferromagnetic electrode with little surface roughness must be prepared. Our AFM measurements showed that 50-nm-thick CMS films grown on 10-nm-thick MgO buffer layers at RT and subsequently annealed at 600 °C had sufficiently flat surface morphologies with rms roughness of about 0.22 nm (Fig. 3). In contrast, AFM measurements showed that as-deposited CMS films had surface morphologies with roughness of 0.34-nm rms. The improved surface flatness revealed by AFM measurement after postdeposition annealing at 600 °C is consistent with the RHEED observations described above.

Fig. 4(a) shows magnetic hysteresis curves up to a magnetic field, H, of 1000 Oe at 300 K for 50-nm-thick CMS films that were as-deposited or postdeposition annealed at 200 to 600 °C. The magnetic field was applied in the plane of the film along

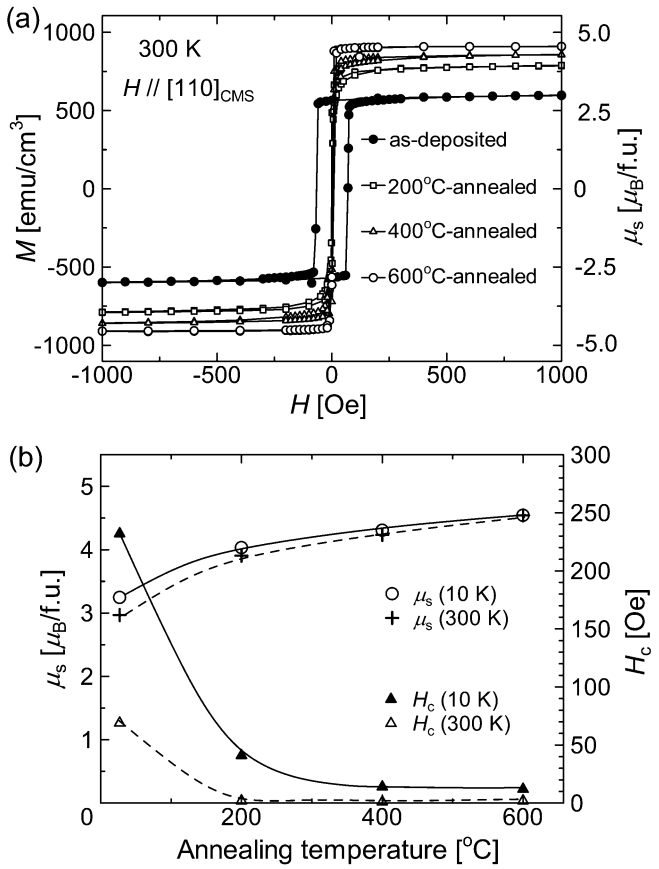

Fig. 4. Magnetic properties of CMS films. (a) Magnetic hysteresis curves up to 1000 Oe at 300 K for 50-nm-thick CMS films as-deposited and postdeposition annealed at 200–600 °C. The magnetic field was applied along the $[110]_{\mathrm{CMS}}$ axis. Magnetization due to the substrate has been subtracted. (b) Annealing temperature dependence of saturation magnetization, μ_{s}, and the coercive force, H_{c}, for 50-nm-thick CMS thin films.

the $[110]_{\mathrm{CMS}}$ axis. Fig. 4(b) shows the annealing temperature dependence of the saturation magnetization, μ_{s}, and the coercive force, H_{c}, for 50-nm-thick thin films at 10 and 300 K. The μ_{s} value of 678 emu cm^{-3} (equivalently 3.2 μ_{B}/f.u.) obtained for the as-deposited films at 10 K increased to 938 emu cm^{-3} $(4.5\,\mu_{\mathrm{B}}/\mathrm{f.u.})$ after postdeposition annealing at 600 °C. Furthermore, the H_{c} value of ∼69 Oe at 300 K for the as-deposited film decreased to less than 5 Oe after annealing at 600 °C. The increase of μ_{s} when postdeposition annealing was applied to the CMS films was probably related to the fact that the crystalline structure changed from the B2 structure or a mixture of the B2 and A2 structures for the as-deposited films to the ordered $\mathrm{L2_1}$ structure after annealing. The A2 structure inevitably contained disorder between the Co and Mn atoms. Theoretical calculation indicated that the disorder between Co and Mn atoms decreased the magnetic moment from that for the $\mathrm{L2_1}$ structure, while the B2-type disorder had little influence [13]. Therefore, by assuming the as-deposited films contained disorder between Co and Mn, we can reasonably attribute the increase of μ_{s} after postdeposition annealing to the appearance of the $\mathrm{L2_1}$ structure. The decrease of H_{c} after postdeposition annealing was also probably related to structural improvement in the sense of the increased 002 and 004 peaks after postdeposition annealing at 400–600 °C. The μ_{s} value of 4.5 μ_{B}/f.u. obtained for the 600 °C-annealed CMS film at 10 K corresponds to about 90% of the theoretically predicted Slater–Pauling value of 5.0 μ_{B}/f.u. for CMS with the $\mathrm{L2_1}$ structure [11].

IV. Summary

We successfully demonstrated the epitaxial growth of $\mathrm{Co_2MnSi}$ thin films with the $\mathrm{L2_1}$ structure on MgO-buffered MgO substrates through magnetron sputtering. The annealed films had sufficiently flat surface morphologies. The saturation magnetization of the annealed films was 4.5 μ_{B}/f.u. at 10 K, corresponding to about 90% of the theoretically predicted Slater–Pauling value for $\mathrm{Co_2}$ MnSi.

Acknowledgment

This work was partly supported by a Grant-in-Aid for Scientific Research (B) (Grant No. 18360143), a Grant-in Aid for Creative Scientific Research (Grant No. 14GS0301) and a Grant-in-Aid for Young Scientists (B) (Grant No.17760267) from the Ministry of Education, Culture, Sports, Science and Technology, Japan.

References

[1] T. Ambrose, J. J. Krebs, and G. A. Prinz, "Epitaxial growth and magnetic properties of single-crystal $\mathrm{Co_2MnGe}$ Heusler alloy films on GaAs," *Appl. Phys. Lett.*, vol. 76, pp. 3280–3282, 2000.

[2] K. Inomata *et al.*, "Large tunneling magnetoresistance at room temperature using a Heusler alloy with the B2 structure," *Jpn. J. Appl. Phys.*, vol. 42, pp. L419–L422, 2003.

[3] T. Marukame *et al.*, "Fabrication of fully epitaxial magnetic tunnel junctions using full-Heusler alloy $\mathrm{Co_2Cr_{0.6}Fe_{0.4}Al}$ thin film and MgO tunnel barrier," *Jpn. J. Appl. Phys.*, vol. 44, pp. L521–524, 2005.

[4] W. H. Wang *et al.*, "Magnetic properties and spin polarization of $\mathrm{Co_2MnSi}$ Heusler alloy thin films epitaxially grown on GaAs(001)," *Phys. Rev. B*, vol. 71, p. 144 416, 2005.

[5] Y. Sakuraba *et al.*, "Huge spin-polarization of $\mathrm{L2_1}$-ordered $\mathrm{Co_2MnSi}$ epitaxial Heusler alloy film," *Jpn. J. Appl. Phys.*, vol. 44, pp. L1100–1102, 2005.

[6] T. Marukame *et al.*, "High tunnel magnetoresistance in epitaxial $\mathrm{Co_2Cr_{0.6}Fe_{0.4}Al}$/MgO/CoFe tunnel junctions," *IEEE Trans. Magn.*, vol. 41, pp. 2603–2605, 2005.

[7] K.-I. Matsuda *et al.*, "Epitaxial growth of $\mathrm{Co_2Cr_{0.6}Fe_{0.4}Al}$ Heusler alloy thin films on MgO(001) substrates by magnetron sputtering," *J. Cryst. Growth*, vol. 286, pp. 389–393, 2006.

[8] M. Yamamoto *et al.*, "Fabrication of fully epitaxial magnetic tunnel junctions using cobalt-based full-Heusler alloy thin film and their tunnel magnetoresitance characteristics," *J. Phys. D*, vol. 39, pp. 824–833, 2006.

[9] T. Ishikawa *et al.*, "Structural and magnetic properties of epitaxially grown full-Heusler alloy $\mathrm{Co_2MnGe}$ thin films deposited using magnetron sputtering," *J. Appl. Phys*. to be published.

[10] S. Ishida *et al.*, "Search for half-metallic compounds in $\mathrm{Co_2MnZ}$ (Z = IIIb, IV, Vb element)," *J. Phys. Soc. Jpn.*, vol. 64, pp. 2152–2157, 1995.

[11] I. Galanakis, P. H. Dederichs, and N. Papanikolaou, "Slater-Pauling behavior and origin of the half-metallicity of the full-Heusler alloys," *Phys. Rev. B*, vol. 66, p. 174 429, 2002.

[12] P. J. Webster, "Magnetic and chemical order in Heusler alloys containing cobalt and manganese," *J. Phys. Chem. Solids*, vol. 32, pp. 0221–1231, 1970.

[13] S. Picozzi *et al.*, "Role of structural defects on the half-metallic character of $\mathrm{Co_2MnGe}$ and $\mathrm{Co_2MnSi}$ Heusler alloys," *Phys. Rev. B*, vol. 69, pp. 094 423-1–094 423-7, 2004.

Manuscript received March 13, 2006 (e-mail: yamamoto@nano.ist.hokudai.ac.jp).